Survival of Organic Materials in Hypervelocity Impacts of Ice on Sand, Ice, and Water in the Laboratory

Mark J. Burchell,[1] Stephen A. Bowden,[2] Michael Cole,[1] Mark C. Price,[1] and John Parnell[2]

Abstract

The survival of organic molecules in shock impact events has been investigated in the laboratory. A frozen mixture of anthracene and stearic acid, solvated in dimethylsulfoxide (DMSO), was fired in a two-stage light gas gun at speeds of ~ 2 and $\sim 4 \, \text{km s}^{-1}$ at targets that included water ice, water, and sand. This involved shock pressures in the range of 2–12 GPa. It was found that the projectile materials were present in elevated quantities in the targets after impact and in some cases in the crater ejecta as well. For DMSO impacting water at $1.9 \, \text{km s}^{-1}$ and 45° incidence, we quantify the surviving fraction after impact as 0.44 ± 0.05. This demonstrates successful transfer of organic compounds from projectile to target in high-speed impacts. The range of impact speeds used covers that involved in impacts of terrestrial meteorites on the Moon, as well as impacts in the outer Solar System on icy bodies such as Pluto. The results provide laboratory evidence that suggests that exogenous delivery of complex organic molecules from icy impactors is a viable source of such material on target bodies. Key Words: Organic—Hypervelocity—Shock—Biomarkers. Astrobiology 14, 473–485.

1. Introduction

IT HAS LONG been debated whether delivery of organic materials from space to young terrestrial planets, such as Earth, played a role in the development of an inventory of complex organic molecules on such bodies (*e.g.*, Chyba and Sagan, 1992, and references therein). Equally, whether this had any influence on the first appearance of life on Earth is also an open question. That complex organic molecules are found in space and can successfully be delivered to Earth is well established. For example, amino acids have been found in meteorites (*e.g.*, the Murchison meteorite, see Cronin, 1989) and Antarctic micrometeorites (Brinton *et al.*, 1998; Matrajt *et al.*, 2004), and polycyclic aromatic hydrocarbons have been found in some interplanetary dust particles (Clemett *et al.*, 1993, or see Sandford, 2008, for a recent review). Large objects in space have also been shown to possess complex organic compounds; for example, dust from comet 81P/Wild 2 has been shown to contain a variety of organic materials (Brownlee *et al.*, 2006; Keller *et al.*, 2006; Sandford *et al.*, 2006), including amino acids, such as glycine, and amines (Glavin *et al.*, 2008). Impacts of comets may thus deliver large quantities of organics in single events. Earth is not the only body to which such materials can be delivered; impacts on Mars may have delivered organics (*e.g.,* Flynn, 1996). Modeling of impacts by cometary icy

bodies on Europa indicates that significant quantities of complex organics may, in some circumstances, be delivered intact (*e.g.*, Pierazzo and Chyba, 1999, 2002).

Once delivered, the next key question concerns survival. To better understand the survival of complex organics in impacts, a variety of laboratory investigations have been undertaken over the years. Impacts from space occur at high speeds and involve sudden heating and extreme shock pressures. Accordingly, some experimenters have applied high temperatures and pressures to organic samples to determine their survivability. For example, Basiuk and Douda (1999, 2001) subjected amino acids to high temperatures to determine survivability, while Peterson *et al.* (1997) subjected amino acids to high-pressure shocks.

A variety of experiments have shown organic synthesis during shock experiments (*e.g.*, McKay and Borucki, 1997) or during hypervelocity impact–generated plasmas (Managadze *et al.*, 2003a, 2003b). It is also possible to fire laser pulses into samples to induce shock effects, and Nna-Mvondo *et al.* (2008) did this with ice targets doped with various materials. They showed that both breakdown and synthesis of organic compounds can occur.

Similarly, some researchers have subjected samples to high-speed impacts using guns. Blank *et al.* (2001) looked at the effect of shock on amino acids by firing flying plates at solutions of amino acids. They found that, as well as

[1]School for Physical Sciences, University of Kent, Canterbury, UK.
[2]School of Geosciences, University of Aberdeen, Aberdeen, UK.

differing survival rates for various amino acids, new peptide bonds could also be formed as a result of the impacts. As well as amino acids, a whole range of organic molecules have been studied. Such impact work can either use organic-rich targets to study shock effects or can fire projectiles containing the compounds of interest at targets. An example of the former is Bowden *et al.* (2009), who froze a suite of organic materials (anthracene, stearic acid, and β,β-carotene) in an ice target and impacted it with stainless steel projectiles at $5\,km\,s^{-1}$. In their experiments, the ejecta from the impacts were found to contain varying fractions of the compounds, depending on angle of ejection, with the more refractory compounds favored at higher angles. Earlier, Burchell *et al.* (2003) had shown that, when frozen in ice targets, even microbes could survive in ejecta thrown off at all angles in impacts at $5\,km\,s^{-1}$.

An example of the use of organic-rich materials as projectiles is given by Bowden *et al.* (2008). They fired mudrock (organic-rich shale) at sand and water targets at speeds of up to $5\,km\,s^{-1}$. Their results show that projectile fragments captured in the targets contained intact organic molecules that could be used as markers of previous biological activity. A more extensive program of impact studies with similar mudrock samples (this time used as both projectiles and targets) was reported by Parnell *et al.* (2010), who found survival of a whole range of organic molecule biomarkers, although there were changes in the thermal maturity of the samples as a result of the impacts.

More quixotically, the behavior of microbial life itself under extreme shocks has been investigated by some groups. Horneck *et al.* (2001) showed in flyer plate experiments that spores in a target could survive a shock of order 32 GPa, albeit with a low survival rate. At the same time, Burchell *et al.* (2001) showed that microbes loaded onto projectiles could survive impacts at $5\,km\,s^{-1}$ (which generate similar shock pressures), again with a low survival rate. Burchell *et al.* (2004) then demonstrated, by varying the impact speed, that in shocks exceeding a few gigapascals, microbial survival falls steeply with a power law; this was later confirmed in flyer plate experiments by Stöffler *et al.* (2007). More recently, Price *et al.* (2013) showed partial survival of yeast spores at speeds up to $7.4\,km\,s^{-1}$. In separate shock recovery experiments, Willis *et al.* (2006) showed that, starting at a few gigapascals, the increased mortality in microbes was due to increasing damage to, and breaking of, cell walls. In an even more adventurous context, Jerling *et al.* (2008) reported on tests for survival of plant seeds fired into water at a few kilometers per second and a few gigapascal shock pressures. They found no survival of viable seeds, with the onset of fragmentation of the seeds at around $1\,km\,s^{-1}$ and 1 GPa. Subsequently, LeVoci *et al.* (2009) reported that in similar experiments they were able to start germination of a seed after it had been fired into water at $1\,km\,s^{-1}$ (roughly 1 GPa peak shock pressure), although they also confirmed the onset of seed fragmentation in most seeds used in impacts at this speed. Separately, in shock experiments, Leighs *et al.* (2012) showed that, at shock pressures approaching 1 GPa, seeds fragment and so are unlikely to survive impacts involving such shocks.

There is thus now an extensive literature on survivability in impacts and extreme shocks. But there is much still to determine. In this current work, laboratory experiments involving hypervelocity impacts of frozen projectiles into a variety of target types are reported. This is partly as analogues of cometary impacts on Solar System bodies and partly uses ice as a convenient delivery system to study the effects of shocks of given peak pressures. The organic content of the frozen projectiles included anthracene and stearic acid. These are organic molecules of differing molecular weights and thermal decomposition temperatures used previously as a target in impact experiments (Bowden *et al.*, 2009); here we test for their successful transfer from ice projectiles to the targets in an impact. The speeds used in this work are around 2 and $4\,km\,s^{-1}$. While somewhat low, they correspond to a range of speeds that covers some specific examples of interest, for example, terrestrial meteorites impacting the Moon (typically 2–$3\,km\,s^{-1}$, see Armstrong, 2010) and impacts on icy bodies in the outer Solar System, for example, impacts on Pluto ($1.9\,km\,s^{-1}$, see Zahnle *et al.*, 2003) and other icy bodies (see Burchell, 2012).

2. Methods

The impacts in this work were obtained by using a two-stage light gas gun (Burchell *et al.*, 1999). Although this gun has been used for many years, it has recently been modified to fire frozen projectiles. The modified gun fires a cylindrical, solid isoplast sabot of external diameter 4.57 mm and 6.5 mm length. A central shaft, width and depth both 4 mm, was drilled in these sabots giving an interior volume of $50.3\,mm^3$. A liquid (see below) was then poured into the hollow shaft, and a cap of quick-setting Araldite epoxy was used to seal the top of the shaft. The filled sabots were then placed in a refrigerator at $-18°C$ until needed. To fire these sabots while still cold required a cold launch tube (into which the sabot was placed) and cold gun breech (which connects the launch tube to the first stage of the gun). Accordingly, before use the launch tube and breech were placed in a freezer and cooled to $-50°C$. When the gun was to be fired, the launch tube and breech were quickly removed from the freezer and placed onto the rest of the gun in the room-temperature laboratory. To slow the rate at which these cold gun parts then warm up, the metal mounts on which they sit were continually cooled to $-18°C$ by flow of coolant circulated from a refrigeration unit. The frozen sabot was then inserted into the launch tube, and the gun was fired. The whole sabot and its contents impacted the target in these shots.

In the shots, projectile speed was measured by passage in free flight of the sabot through two laser light curtains focused onto photodiodes. The output of the photodiodes was captured on a fast oscilloscope, and the time between then combined with their known separation gave the speed. The speed of each shot was controlled by selection of the gas used in the two-stage gun. During a shot, the range of the gun was evacuated to < 1 mbar, unless the target was water, in which case the gun was fired when the pressure had fallen to 50 mbar.

Two types of liquids were frozen in the sabots in this work. The first was commercial black ink (Quink). Quink is a well-known commercial ink. It was used as a test material and marker to show the likely spread of materials after impact. The second was a mixture of anthracene and stearic

acid, solvated in dimethylsulfoxide (DMSO). These materials were chosen because they cover a range of properties. Stearic acid has both biological and abiological origins and has a long chain structure. It also has a thermal decomposition temperature in the range of 190–400°C. Anthracene, which has an abiological origin, is relatively stable at high temperatures and has a thermal decomposition temperature of over 400°C, although it should be noted that at standard conditions it has a boiling point of 340°C. DMSO is a widely used solvent and is highly miscible. It has a freezing point of 18.5°C

Three types of target (water, ice, and sand) were used as indicative of various surfaces found in the Solar System. The water targets used reverse-osmosis purified water, placed in a thin-walled, water-rich, plastic bag. The front-to-back thickness of the filled bag was 33.4 mm, but in some shots the target was rotated by 45° to the direction of flight of the sabot, giving an effective maximum water depth along the line of flight of 47.2 mm. The volume of water used in a shot was approximately 195 cm^3. The bag was mounted in a target holder used in earlier work with water targets (see Milner *et al.*, 2006, and Baldwin *et al.*, 2007). The bag was fixed to a stand that held the bag vertical, with a near-flat front face and flat rear face, and could be rotated with respect to the impact direction (Fig. 1a). When in the gun, the stand was placed in a tray with a box over the top to contain any water that was spilled in the impact. The water bag was fully contained by this setup except for a small opening in the box to permit entry of the projectile. The stand, tray, and box were cleaned with isopropanol alcohol between shots.

The sand was placed in a similar plastic bag with the same depth as the water. In the sand shots, the impacts were at 45° to normal incidence. The sand was a quartz-rich sand from the Lower Greensand, Leighton Buzzard, Beds, UK. The supplier claimed it was relatively free from silt, clay, and organic matter. However, earlier work with similar sand had shown traces of organic contamination. Accordingly, in the present study, the sand was sonified for 20 min and then heated in an oven to 100°C to dry before use. The grain size was 0.6–1.18 mm, and the grains were semi-rounded in shape.

The ice targets were made from crushed grains and flakes of ice. These were typically a few millimeters in size and made a target 20 cm deep with porosity of approximately 50%. Impacts on the ice targets were at normal incidence, and the ice was at approximately −50°C. In the ice shots, it was anticipated that there would be significant amounts of ice ejected from the target during the impacts. Therefore, the floor of the target chamber was lined with an insulating sheet that was used to collect the ejecta, which could then be sampled for subsequent analysis.

After each shot, samples of the target material were collected for analysis. The samples were initially screened in a two-stage process designed to minimize potential contamination. Because of the small volumes the ice projectiles carried within each sabot, the potential for loss of analyte or contamination during sample processing was high compared to previous work on ice targets that were doped with similar compounds (Bowden *et al.*, 2009). To this end, the number of stages of sample processing was kept to a minimum, and a number of analytical controls and blanks were utilized to monitor each stage, including volume reduction and the extraction of sand targets.

Prior to analysis, samples of aqueous targets (crushed ice and bags of water) had their volume reduced (samples were reduced to near dryness at the edge of a fume hood in a clean analytical facility at ambient temperature ∼18°C). Sample containers were then rinsed with redistilled methanol and dichloromethane to transfer contents to small glass vials. Analytes were recovered from samples of the sand target by sonication in organic solvents. Sonication was performed for 5 min in methanol, 5 min in 1:1 (volume:volume) methanol:dichloromethane, and 5 min in dichloromethane. The combined solvents were then reduced to dryness at ambient conditions by placing them in a fume hood and then transferred to small vials.

The DMSO, anthracene, and stearic acid present were analyzed by gas chromatography–mass spectrometry. Analyses
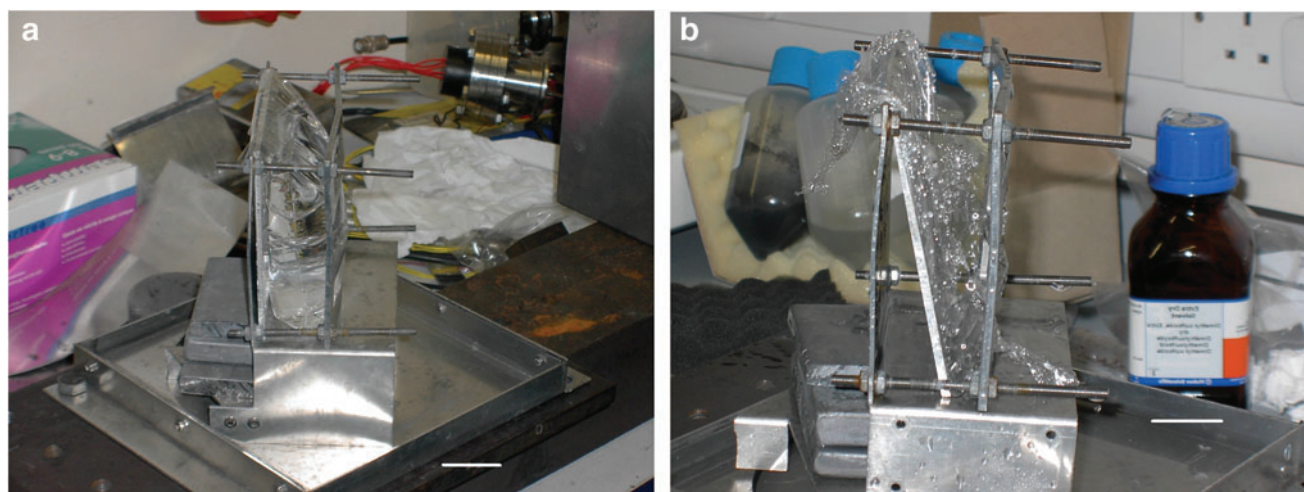

FIG. 1. Target holder with water target. (**a**) Pre-shot. (**b**) Post-shot. Note that in these images the surrounding box has been removed. Impact direction was from the right. A 3 cm scale bar is shown in the bottom right of both images. (Color images available online at www.liebertonline.com/ast)

were performed on an Agilent 6890N gas chromatograph, fitted with a J&W DB-5 phase 50 m length, 0.25 mm i.d., and 0.25 μm film thickness column. This was connected to a 5975 MSD quadrupole mass spectrometer. Analyses were performed on underivatized samples and the same samples subsequently derivatized with BSTFA (N,O-bis(trimethylsilyl) trifluoroacetamide). The gas chromatograph oven temperature program was 30°C, for 5 min rising at 3°C/min to 170°C, then rising at 4°C/min to 295°C, and holding for 26 min. A key aspect of the analytical procedure was also the temperature program for the programmed-temperature vaporizing injector. This was 20°C for 2 min, before a ballistic heating stage (instrument raises temperature as quickly as possible) raised the temperature to 300°C. The injector was operated in splitless mode and purged after 65 min. Prior to manual injection, samples were kept at ~50°C.

Although the mass spectrometer was operated in scan mode, compounds were principally identified by their relative retention times compared to analyses of standard compounds. An internal standard of D4 cholestane was added prior to analysis and used for quantification. The following response factors, relative to D4 cholestane, were used (the m/z 221 ion was used to measure D4 cholestane): DMSO relative response factor (RRF) = 1.6 for $m/z = 78$; anthracene RRF = 0.58 for $m/z = 178$; BSTFA-derivatized stearic acid RRF = 1.3 for m/z 341. Based on the measurement of noise peaks in the vicinity of target compounds on their diagnostic ion chromatograms, we estimate minimum sensitivity to typically be between 10^{-6} and 10^{-7} micrograms per milligram of water for anthracene and stearic acid. For DMSO, it was typically 10^{-6} micrograms per milligram of sample. The variability from run to run was ±10% in the worst cases, with DMSO showing the most variation depending on the concentration involved. For DMSO, the variability was kept low by ensuring that injector temperatures were steady prior to the beginning of an analysis.

3. Results of Impact Experiments

Six shots were carried out; the shot program is given in Table 1. The two shots with black ink tested the setup and provided experience in handling the materials. Two basic speeds were used, approximately 2 and 4 km s^{-1}. Three of the shots were at normal incidence, as usual in laboratory experiments. However, in addition, three impacts were made at an inclined incidence of 45°, simulating the typical im-

pact angle in space. Although the magnitude of the impact speed is unchanged, the vertical component is reduced, and this in turn gives a reduced peak shot pressure (see Pierazzo and Melosh, 2000a, for a discussion).

The ink shot into water was the first shot carried out, and the sabot hit the target at 2.0 km s^{-1}. After the shot, it was observed that the plastic bag holding the target water had split during the impact and that most of the water had flowed into the mounting tray (see Fig. 1). All the water was collected after the shot and poured through a Watman 200 filter paper. The filter paper was then allowed to dry, and it was found that it was stained with black ink (Fig. 2). Previous shots made into water without ink in the projectile do not show such staining. This shows, in principle, that at 2 km s^{-1} at least some of the frozen sabot contents can be transferred to a water target and detected after impact.

The second ink shot was into a crushed ice target (Fig. 3) at 4.39 km s^{-1}. The target was examined after impact, and the front surface around the impact point was found to have been removed in the impact. The central point of the impact was identified by the presence of a bright, white region in the ice (Fig. 3b), which past experience has shown to be characteristic of the bottom of the central pit in an ice target after impact. The surrounding ice surface showed some general discoloration due to gun debris that is often found in these shots. However, in addition, the exposed ice surface also showed signs of black ink over a region some 8 cm across (Fig. 3b). This did not fully surround the central pit in the crater but, in Fig 3b, is seen above and to the right of the central pit. There was fainter visual evidence of a small amount of ink to the left of the central pit, but this does not show up in the image in Fig. 3b, as it was hard to photograph. Overall, we concluded that the ink was present in observable quantities in the surface region of the exposed ice to a radial distance of some 4 or 5 cm from the central impact point.

The next set of shots used the DMSO, anthracene, and stearic acid solution loaded in the sabot. The first of these shots fired the frozen sabot at 1.97 km s^{-1} into a water target similar to that in Fig. 1a. After the shot, it was observed that the bag containing the water had split as before and most of the water was in the tray beneath the bag. This was collected in sterile containers for subsequent analysis. After a shot, the target chamber of the gun is brought back to atmospheric pressure, and then air flows through for 10 min to purge any vapors in the chamber that arose from the firing of the gun. In this shot (and in all the others in this work featuring the DMSO, anthracene, and stearic acid mixture), there was a rich, burnt organic smell still present after the target chamber was opened. This smell is not normally present after a shot.

The shot into sand used the same setup as those into water, with the sand placed in the target holder in the same way that the water had been (Fig. 4). After impact, it was again observed that the bag containing the sand was torn, but not to the same degree as in the water experiments, and a noticeable amount of the sand was still in the lower part of the bag. The sand that had flowed out of the bag had two destinations: some flowed out and sat on a ledge just in front of the bag; the rest was distributed over the floor of the tray (Fig. 4b). All these regions were sampled separately, and the collected sand was stored for analysis. During the sampling, it was noticed

TABLE 1. SHOT PROGRAM

Shot	Projectile contents	Target type	Impact speed (km s^{-1})	Impact angle
1	Black ink (Quink)	Water	2.00	Normal
2	Black ink (Quink)	Crushed ice	4.39	Normal
3	DMSO + anthracene + stearic acid	Water	1.97	45°
4	DMSO + anthracene + stearic acid	Sand	1.98	45°
5	DMSO + anthracene + stearic acid	Crushed ice	4.19	Normal
6	DMSO	Water	1.90	45°

FIG. 2. Ink on filter paper after passage of water from target impacted at $2.00\,\mathrm{km\ s^{-1}}$ by a sabot containing frozen ink.

that a fine, white powder covered some of the sand in the tray. This powder was also collected. Some of it was imaged optically, and some was examined in a scanning electron microscope (SEM) (images in Fig. 5). The SEM work also permitted an elemental analysis and showed that the powder was fine fragments of the original sand that had been broken up during the impact. As can be seen in Fig. 5, as expected not only were the fragments of the sand grains smaller than the original grains, but they also possessed the sharper, angular features associated with fragmented rock targets.

The next shot was onto a crushed ice target at $4.19\,\mathrm{km\ s^{-1}}$ in which the DMSO, anthracene, and stearic acid mixture was used. The sabot was frozen as usual. The target and its ejecta after impact are shown in Fig. 6. In Fig. 6a, a bright white region in the center of the target marks the center of the impact crater. Some of the ice from this region then fell to the bottom of the container, where it could be seen. Ice was also thrown off the target as impact ejecta and traveled down the target chamber (Fig. 6b). After the shot, the surface of the ice target was examined for signs of discoloration (the DMSO in the projectile had a strong orange color), but none was observed. However, it should be noted that dropping drops of the liquid DMSO, anthracene, and stearic acid solution directly onto a test ice target produced only mild discoloration that faded on a timescale of just a few minutes, so we would expect to see no discoloration in our ice target after its removal from the gun. Samples (typically 20–40 mL) were taken for analysis from several
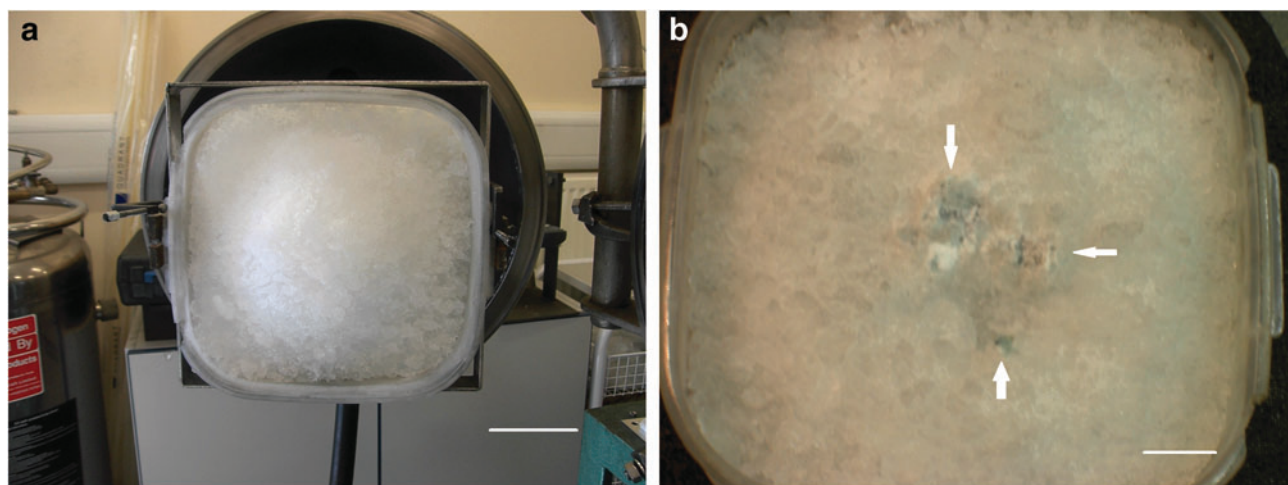

FIG. 3. The surface of a porous ice target (**a**) mounted in the door of the gun pre-shot and (**b**) after impact at $4.39\,\mathrm{km\ s^{-1}}$ by a sabot containing frozen black ink. In (b) regions of intense black ink are shown with arrows. The center of the impact crater is in the middle of the image where a small white circular feature can be seen (this is characteristic of the central pit in impact craters on ice in the laboratory). The scale bar shown in 3a is 5 cm, and that in 3b is 2 cm. (Color images available online at www.liebertonline.com/ast)
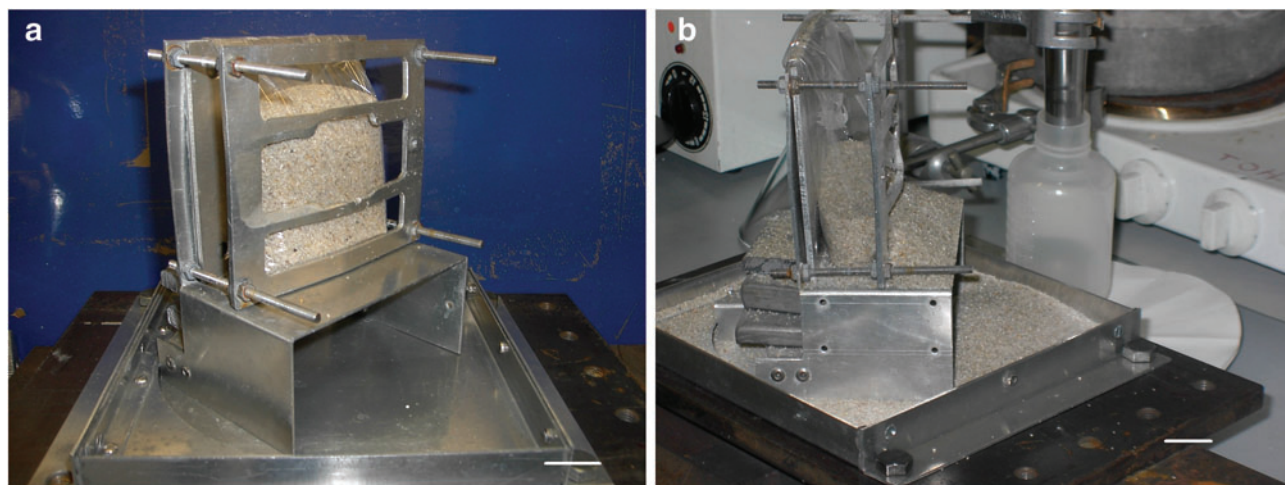
FIG. 4. Target holder filled with sand. (**a**) Pre-shot. (**b**) After impact at 1.98 km s^{-1} by a sabot containing frozen DMSO, anthracene, stearic acid, and β,β-carotene (the impact direction was from the right). In (b) it can be see that, after the impact, some sand was retained by the lower part of the bag, but the rest flowed out onto the holder and the tray underneath. Scale bars are shown in the bottom right of both images and represent 2 cm. (Color images available online at www.liebertonline.com/ast)
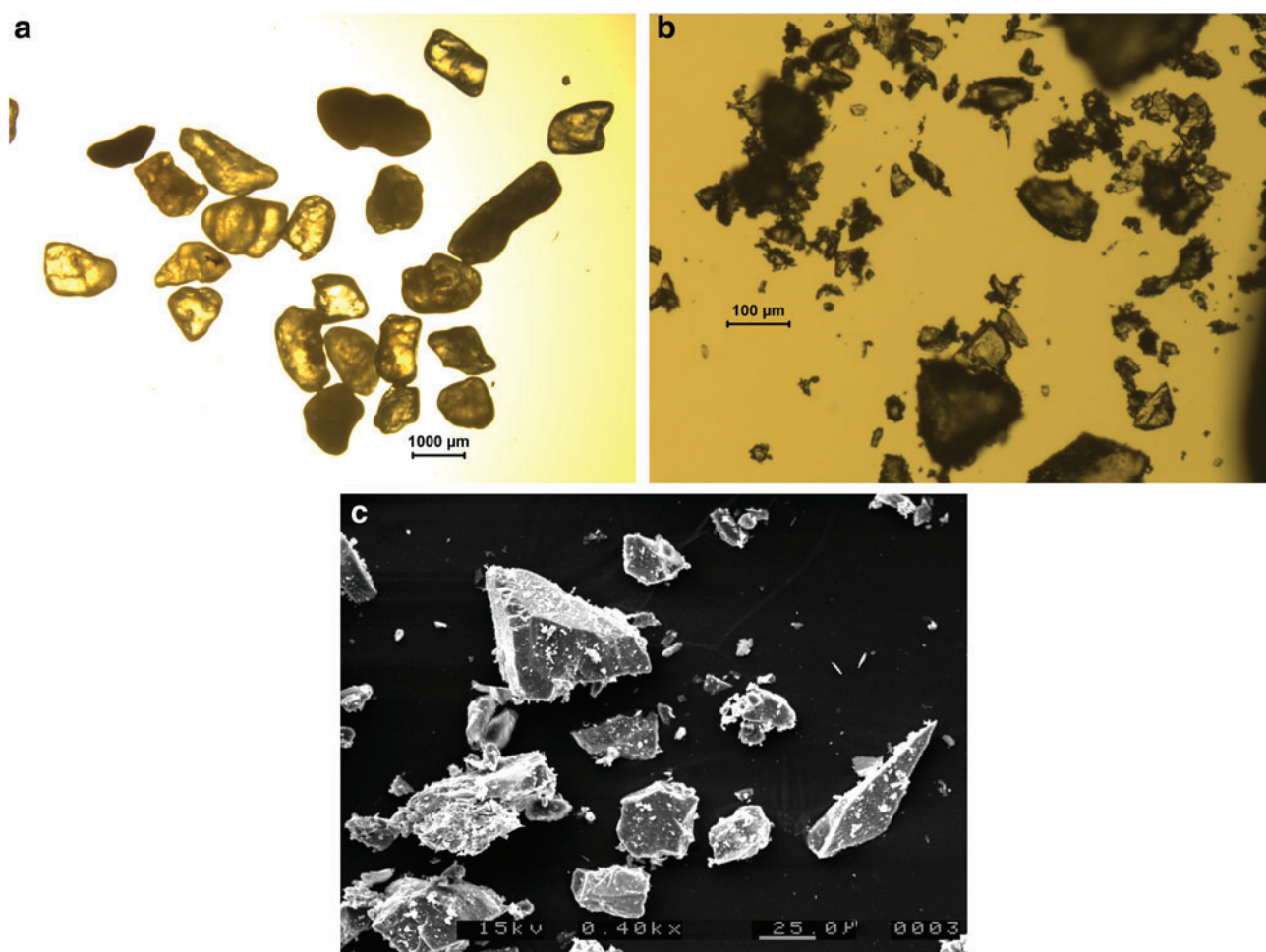
FIG. 5. Images of sand grains used in this work. (**a**) Optical image pre-shot. (**b**) Optical image post-shot, showing presence of fragments of various sizes. (**c**) SEM image post-shot. Note the evolution in size scales in each image, from the 1000 μm scale bar in (a) to 100 and then 25 μm in (b) and (c), respectively. (Color images available online at www.liebertonline.com/ast)

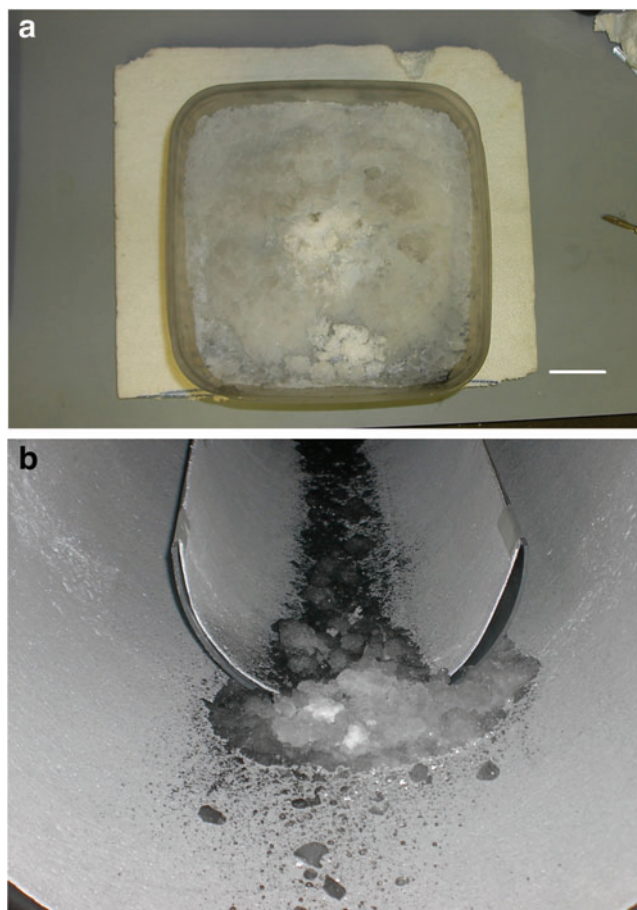**FIG. 6.** (**a**) Crushed ice target after impact at 4.19 km s^{-1} by a sabot containing frozen DMSO, anthracene, stearic acid, and β,β-carotene. (**b**) The ice ejected from the target in (a) during the shot was collected in the floor of the target chamber. Some of the ejecta was blackened during the impact by gun debris, but some was a particularly bright white just like the ice in the center of the crater in the target. The scale bar shown is 3 cm. (Color images available online at www.liebertonline.com/ast)

regions of the ice target. The bright white central area was sampled, the area around it out to about 5 cm was sampled (following the experience gained from the shot with ink), and a region in the corner of the target surface, some 20 cm away from the impact point, was also sampled for completeness. Two samples were taken from the ejecta. The white ice (see Fig. 6b) was sampled, and a separate sample of the blackened dirty ice was also taken.

The final shot was of a sabot loaded with just DMSO. This was to enable an absolute measurement of the survival of one material in an impact. The impact speed was 1.90 km s^{-1}, and the impact was at 45° from the normal. The water was collected as in the earlier shot and analyzed for its DMSO content. This was compared to a sample of the target water taken just before the shot.

4. Results of Sample Analysis

As already stated, at the same time as the shots were performed, a drop test was carried out by using liquid from the same batch of DMSO, anthracene, and stearic acid. In the drop test, liquid was dropped from a pipette onto an ice

target, and the ice was observed to be stained. This staining then rapidly faded. The volume of the drop in a test was similar to the contents of the sabot used in the separate shots. Ice from the stained area totaling 10 mL was sampled and analyzed per the analysis chain described above. We also ran control samples of the ice taken from the target before the drop test. The results are presented in Fig. 7 and show a significant increase (of typically 2–3 orders of magnitude) in the concentration of each of the materials (DMSO, anthracene, and stearic acid). Since there is no significant shock involved, this is not unexpected, but it does show that the analysis method was sensitive to the quantities used.

The results of the shot into water at 1.97 km s^{-1} are shown in Fig. 8. The concentrations in the water of the three organic materials fired in the projectile show large and very significant increases after the shot (by 5–7 orders of magnitude).

The results of the shot into sand at 1.98 km s^{-1} are shown in Fig. 9. The control sample was a fraction of the sand that was not used in the shot. The sand used as the target was sampled several times for the analysis after the shot. After the shot, some sand remained *in situ* in the original bag; this is referred to as "Target post-shot" in Fig. 9. Sand that had fallen from the original target and rested just in front of it was labeled "Ejecta A," and sand that had scattered widely was referred to as "Ejecta B." This time not all the projectile materials showed up at elevated levels in the target after impact. The anthracene concentration was roughly constant or even fell by an order of magnitude. As already stated, anthracene has a high thermal decomposition temperature (>400°C, although at standard pressure it boils at 340°C) but either did not survive or was proved more volatile than the other materials used. By contrast, the stearic acid and DSMO were both seen in greatly enhanced concentrations in the ejecta.
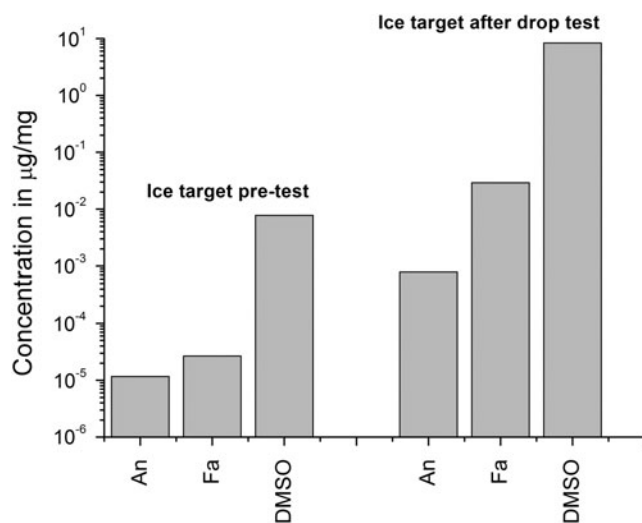

FIG. 7. Results of analysis of target ice material before (left-hand grouping of data) and after (right-hand grouping of data) drop test. The data shows the concentration of the named material in terms of microgram (of material) per milligram of sample tested. An is anthracene, Fa is stearic acid, and DMSO is dimethylsulfoxide.
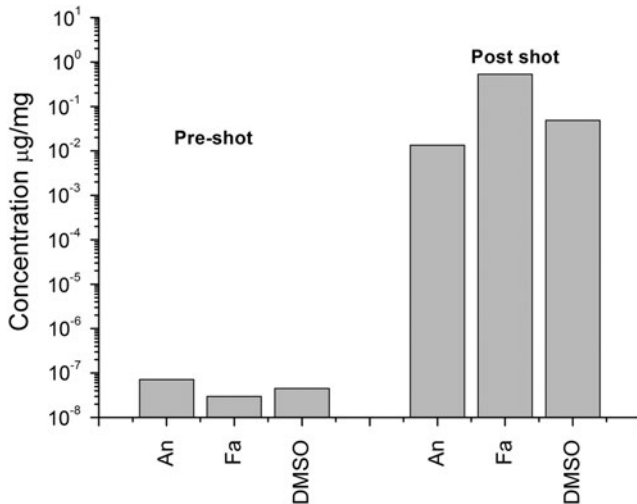
FIG. 8. Results of analysis of water, before and after use as the target in the impact at 1.97 km s^{-1} and 45° incidence. The left-hand group of data are for the water in the target sampled ''Pre-shot''; the right-hand group of data are for water sampled from the target ''Post-shot'' (*i.e.*, after the impact). The data show the concentration of the named material in terms of microgram (of material) per milligram of sample tested. An is anthracene, Fa is stearic acid, and DMSO is dimethylsulfoxide.
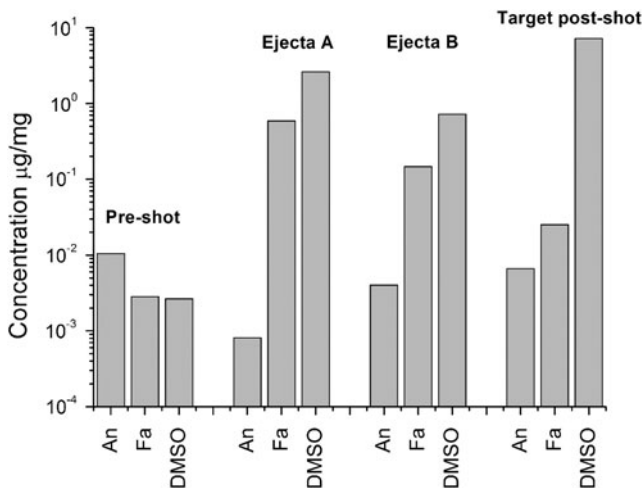

FIG. 9. Results of analysis of sand before and after use as a target in an impact by an ice-filled sabot at 1.98 km s^{-1} and 45° incidence. The ''Pre-shot'' values are those from a fraction of the sand that was not used in the shot. The data show the concentration of the named material in terms of microgram (of material) per milligram of sample tested. An is anthracene, Fa is stearic acid, and DMSO is dimethylsulfoxide. Sand from three locations was analyzed after the impact. Sand sampled from the sand that remained in the original target bag after the impact is labeled ''Target post-shot.'' Samples from sand that fell from the bag during the impact and was located just in front of it is labeled ''Ejecta A.'' And the sample from sand that was scattered widely by the impact is labeled ''Ejecta B.''

The concentration of DSMO was also significantly increased in the target itself post-shock.

At the higher speed of 4.19 km s^{-1}, the impacts on ice again showed (Fig. 10) that the center of the crater had significantly enhanced levels of all three materials (anthracene, stearic acid, and DMSO) post-shot. In the ejecta collected from the floor of the target chamber after the shot, only stearic acid was found at significantly elevated levels, at a concentration about 3 orders of magnitude above that of the control but an order of magnitude less than in the center of the crater. The concentration of DMSO was similar to that in the original ice. However, we did not find anthracene at detectable levels.

The final shot was of a sabot that was loaded just with DMSO into a water target (impact speed 1.90 km s^{-1} and at 45° incidence). The DMSO content of the target water was measured pre-shot and compared to that obtained after the impact (see Fig. 11). As in the earlier shot into water (Fig. 8), there was significant enhancement of the DMSO content post-shot. The post-shot sample of water was analyzed in two separate runs, and the variability was found to be ±10.8%. The volume of the DMSO that was loaded in the sabot was measured (55.3 mg) pre-shot, and the volume of target water used was also monitored (328 mL). Combined with the concentration of DMSO in the water post-shot, this suggests that 24.2 ± 2.6 mg of DMSO successfully transferred to the target in the impact, a surviving fraction of 0.44 ± 0.05.

5. Peak Shock Pressures

To estimate peak shock pressures in the impacts, we began by using the planar impact approximation (PIA) (see
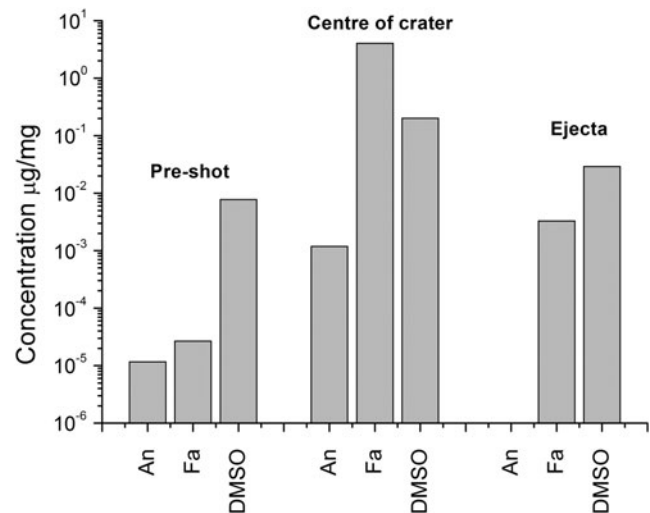

FIG. 10. Results of analysis of the ice target in an impact at 4.19 km s^{-1} and normal incidence. The data show the concentration of the named material in terms of microgram (of material) per milligram of sample tested. The ''Preshot'' (left-hand group of data) is the ice sampled before it was used in the impact. The data labeled ''Centre of crater'' were removed after the shot from the floor of the impact crater formed in the impact. The data labeled ''Ejecta'' were taken from the ejecta captured after the shot in the target chamber away from the target. An is anthracene, Fa is stearic acid, and DMSO is dimethylsulfoxide.
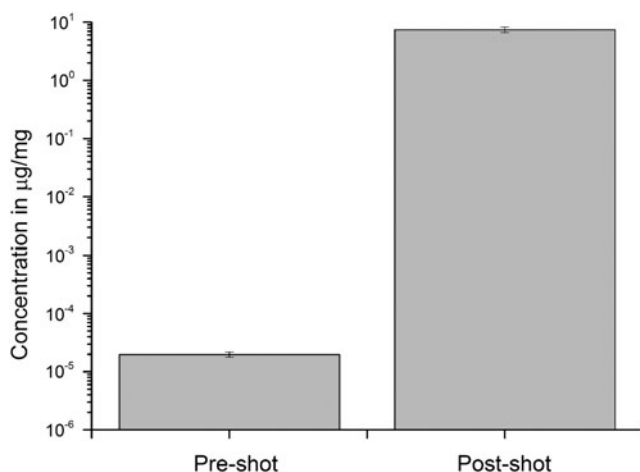
FIG. 11. Concentration of DMSO in water, before and after use as the target in the impact at $1.90 \, \text{km s}^{-1}$ and 45° incidence. The projectile contained only DMSO. The analysis of the water was repeated and was reproducible to $\pm 10.8\%$.

Melosh, 1989, for an explanation). This is an analytical solution of the peak pressure based on linear wave speed relations in each material (the values used in the linear wave speed relations are given in Table 2) and solving the shock conditions across a boundary between two semi-infinite planes. As such it estimates the peak shock pressure near the projectile:target plane. In the interior of the projectile, the peak pressure will vary with location, typically falling to half the peak value in the median plane of the impactor and having a mean value approximately ¼ of the peak value in the trailing (rear) half of the impactor (see Parnell *et al.*, 2010, for a discussion). Given the unusual nature of the projectile contents (a mixture of organic molecules), we approximated this as water ice in the calculations. Further, given the mixed composition of the impactor (a nylon and frozen ice projectile), we estimated the pressures twice, once assuming a solid nylon projectile and once assuming the projectile was just water ice. For non-normal incidence, we applied the result of Pierazzo and Melosh (2000b), who estimated that peak pressures fall with sine of the angle of incidence. In the case of the ice target, the impactor was slightly smaller or a similar size to the ice grains, and accordingly rather than make an *ad hoc* adjustment for porosity, we made the approximation that the target was nonporous ice. The results (Table 3) are thus approximate but do give an indicative range of peak pressures in each event.

TABLE 2. LINEAR WAVE SPEED EQUATION
COEFFICIENTS FOR $U = C + SU$

Material	C(km s⁻¹)	S	Density (kg m⁻³)	Reference
Ice	2.3	1.31	910	Senft and Stewart, 2008
Water	1.48	1.60	1000	Melosh, 1989
Sand	1.70	1.31	1600	Melosh, 1989
Nylon	1.63	2.29	1184	Matuska, 1984

Additionally, we used ANSYS' AUTODYN hydrocode (Hayhurst and Clegg, 1997) to independently determine the peak pressure. All simulations were modeled in three dimensions by using a Lagrangian method, with 10 cells across the radius of the projectile (giving a total of $\sim 500,000$ cells in total). Peak pressures were determined by placing tracers (referred to as ''gauges'' in AUTODYN) within the projectile. Figure 12 shows a set of time frames from a simulation of the impact at $4.39 \, \text{km s}^{-1}$. The presence of the shock waves reflected from the sabot walls into the ice projectiles increases the peak pressure by about 30%. The peak pressures experienced during the impacts for the five shots are also given in Table 3 and occur just behind the front plane where contact between projectile and target occurs. The simulated peak pressures are similar to those found by using the PIA, giving additional confidence that the pressures calculated with either method are close to reality. Standard AUTODYN library materials were used to simulate water (Trunin *et al.,* 2001), sand (Laine and Sandvik, 2001), and nylon (Matuska, 1984). Ice was simulated by using the 5-phase EoS detailed by Senft and Stewart (2008), who used an easy-to-implement strength model validated against experimental data described by Fendyke *et al.* (2013). The duration of the shock in a sample is illustrated in Fig. 13 for an individual gauge point in the ice part of a projectile in one impact. The peak pressure lasts of order 20 ns and then falls over $1.5 \, \mu s$ to 20% of its peak value.

Taken together, these calculations indicate that the peak shock pressures in the shots at $\sim 2 \, \text{km s}^{-1}$ were of order 2–4 GPa, while in the shots at $\sim 4 \, \text{km s}^{-1}$ they were of order 6–16 GPa.

6. Observations and Conclusions

The results show that, at pressures in the range up to around 15 or 16 GPa, the materials used can successfully transfer from an impactor to the target in a high-speed impact. In addition, material was also found in the impact ejecta. In the case of impacts on water at $1.90 \, \text{km s}^{-1}$ (shock pressures around 2–4 GPa), we found that $44\% \pm 5\%$ of the DMSO survived after impact.

It should be noted, however, that not all the materials survived the transfer from projectile to target in all cases. In two of the examples here, it was observed that anthracene did not transfer to either the target or ejecta, or was potentially destroyed by the impact process. Such selective effects have been observed before. For example, when targets were doped, pre-shot with anthracene, and then impacted by inert projectiles, anthracene was only observed in ejecta at intermediate and high angles and not at shallow angles (see Bowden *et al.*, 2009). There is also evidence from recovery impact experiments (where fragments of the projectile are recovered from the target after an impact) that thermal processing occurs during impacts and can change the organic content of projectile fragments recovered after impact experiments at speeds of $1–5 \, \text{km s}^{-1}$ (*e.g.*, see Bowden *et al.*, 2008, and Parnell *et al.*, 2010).

That material can survive high-speed impacts from space is well established. On Earth, meteorites that slowed during passage through the atmosphere have been recovered, as have impactor fragments from large high-speed

Table 3. Peak Shock Pressures Estimated Using the Planar Impact
Approximation (PIA) and AUTODYN Hydrocode

Shot	Target	Impact speed (km s^{-1})	Impact angle	Peak pressure (PIA: ice projectile) GPa	Peak pressure (PIA: nylon projectile) GPa	Peak pressure (AUTODYN) GPa
1	Water	2.00	90°	3.3	3.9	3.47
2	Ice	4.39	90°	7.5	13.1	15.8
3	Water	1.97	45°	2.3	2.7	2.28
4	Sand	1.98	45°	2.7	3.3	2.49
5	Ice	4.19	90°	7.0	12.1	14.6

impacts. For example, on land, analyses of drill cores at the Morokweng impact site have revealed 25 cm sized asteroid clasts (Maier *et al.*, 2006), and Kyte (2002) reported unmelted fragments that were recovered from the ocean floor at the Eltanin impact site. These impacts would have been at higher speeds than those in the experiments here, but the recovery of material after an impact is still demonstrated. In determining whether such material can contain viable organic molecules, it is often not only elevated temperatures that are critical but also the peak shock pressures that were endured. It should, however, be remembered that the shock duration in the experiments here, and any accompanying elevated temperatures, for example, are of shorter duration than those that occur in a planetary-scale impact.

There are other places in the Solar System where impacts occur and which will feature speeds similar to those used here. For example, giant impacts on Earth can launch ejecta that would impact the Moon (see Armstrong *et al.*, 2002).

The typical speed of these lunar impacts would be of order 2–3 km s^{-1}, and the impacts would not be vertical (Armstrong, 2010). The impact speeds and angles are thus directly comparable to those used here (although, of course, the impactor will be rocky not icy). In the outer Solar System, impact speeds will be lower, with typical impact speeds on Pluto of 1.9 km s^{-1} (Zahnle *et al.*, 2003). For impacts on the icy satellites of the outer planets, impact speeds can be rather high, as the contribution from the infall speed of the parent planet can be large for a body approaching from interplanetary space. Lower speeds can, however, occur for material exchanged between the icy satellites of a parent planet. This can aid interchange of material between such bodies, in the manner of the icy panspermia referred to by Burchell *et al.* (2003).

Thus in a variety of ways we can envisage impacts in the Solar System at similar speeds and shock pressures to those used here. In addition, in the cases involving outer Solar System bodies, the impactors may be icy. Either way, if the
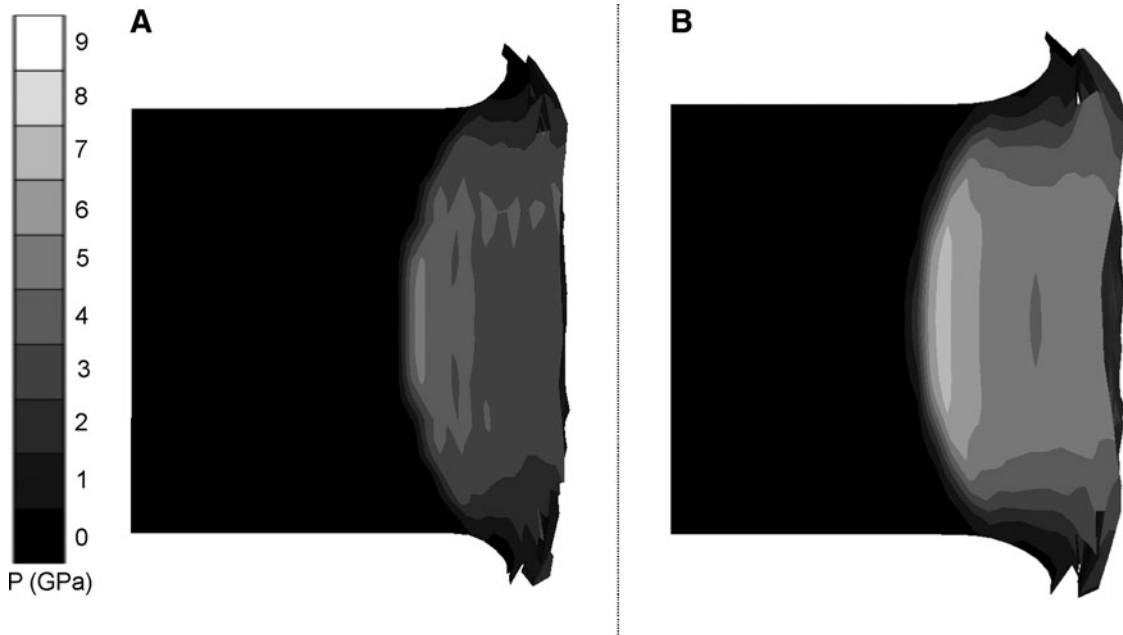

FIG. 12. Pressure contour cross section through center of projectile (the target has been removed for clarity) in an impact at 4.39 km s^{-1} onto ice. (**A**) gives the pressure of a solid ice projectile 0.7 μs after impact. (**B**) shows the pressure if we contain the ice within a nylon projectile (as was actually shot). There is an enhancement of the pressure by approximately 30% due to reflection of a pressure wave off the internal wall of nylon casing. Therefore, we estimate a 30% enhancement in the peak shock pressure due to reflection off the containing nylon casing.
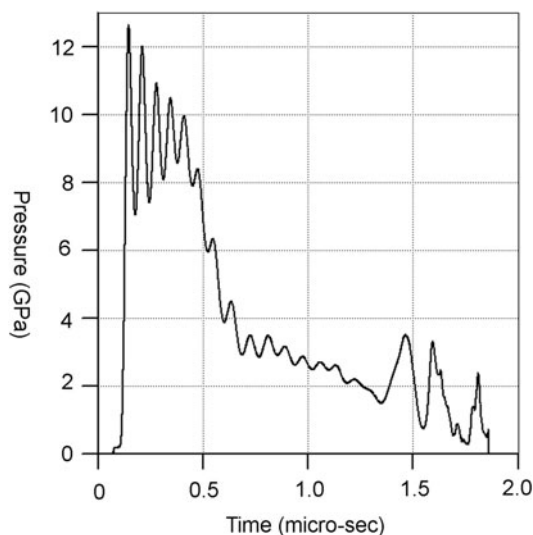
FIG. 13. Pressure versus time for a gauge point located just below the front surface of the ice projectile that experienced the peak pressure ($\sim$12 GPa) for approximately 20 ns before decaying to $\sim$2 GPa on the timescale of 1.5 μs.

impactors contain biomarkers such as those used here, then under similar shock pressures we can predict survival of significant quantities of these biomarkers. The exact surviving fraction is hard to quantify here, however, due to only partial sampling of the target material, and we will explore this further in future experiments.

What is shown here experimentally is that survival and successful transfer of organic biomarkers to targets does indeed occur in high-speed impacts. This complements previous work on the subject. For example, Blank *et al.* (2001) reported on shock experiments on samples of amino acids in aqueous solution. They used a flier plate launched in a gun to shock their sealed samples to peak pressures of between 5.1 and 21 GPa, overlapping the pressure regime here. They found that a large fraction of amino acids survived in all their experiments, although there were differences in survival rates between different amino acids. In other experiments, Bertrand *et al.* (2009) subjected saponite clays to pressures in the range of 12–28.9 GPa. They found survival, though differences appeared in survival rates as the shock pressure increased, namely, that amino acids with an alkyl side chain were more likely to survive than those with functional side chains.

The work here directly complements that of Bowden *et al.* (2009), who showed that viable organic compounds frozen in ice could be ejected in high-speed impacts. What is shown here is that such material can then impact a new body and successfully transfer to it. Indeed, some of the incident material in our work was then found in the ejecta from the impact craters. Pierazzo and Chyba (1999, 2002) modeled amino acid survival in impacts at higher impact speeds. Their work used hydrocodes to simulate kilometer-sized bodies impacting targets at speeds up to 30 km s^{-1}. They predicted that, under the right impact conditions, survival could occur even at these high speeds. Overall, there is thus a growing body of evidence that supports survival of complex organic material in hypervelocity impacts typical of those in the Solar System.

Author Disclosure Statement

No competing financial interests exist.

Abbreviations

DMSO, dimethylsulfoxide; PIA, planar impact approximation; RRF, relative response factor; SEM, scanning electron microscope.

References

Armstrong, J.C. (2010) Distribution of impact locations and velocities of Earth meteorites on the Moon. *Earth Moon Planets* 107:43–54.

Armstrong, J.C., Wells, L.E., and Gonzalez, G. (2002) Rummaging through Earth's attic for remains of ancient life. *Icarus* 160:183–196.

Baldwin, E.C., Milner, D.J., Burchell, M.J., and Crawford, I.A. (2007) Laboratory impacts into dry and wet sandstone with and without an overlying water layer: implications for scaling laws and projectile survivability. *Meteorit Planet Sci* 42: 1906–1914.

Basiuk, V.A. and Douda, J. (1999) Pyrolysis of simple amino acids and nucleobases: survivability limits and implications for extraterrestrial delivery. *Planet Space Sci* 47:577–584.

Basiuk, V.A. and Douda, J. (2001) Survivability of biomolecules during extraterrestrial delivery: new results on pyrolysis of amino acids and poly-amino acids. *Adv Space Res* 27:231–236.

Bertrand, M., van der Gaast, S., Vilas, F., Horz, F., Haynes, G., Chabin, A., Brack, A., and Westall, F. (2009) The fate of amino acids during simulated meteoritic impact. *Astrobiology* 9:943–951.

Blank, J.G., Miller, G.H., Ahrens, M.J., and Winans, R.E. (2001) Experimental shock chemistry of aqueous amino acid solutions and the cometary delivery of prebiotic compounds. *Orig Life Evol Biosph* 31:15–51.

Bowden, S.A., Court, R.W., Milner, D., Baldwin, E., Lindgren, P., Crawford, I., Parnell, J., and Burchell, M.J. (2008) The thermal alteration by pyrolysis of the organic component of small projectiles of mudrock during capture at hypervelocity. *J Anal Appl Pyrolysis* 82:312–314.

Bowden, S.A., Parnell, J., and Burchell, M.J. (2009) Survival of organic compounds in ejecta from hypervelocity impacts on ice. *International Journal of Astrobiology* 8:19–25.

Brinton, K.L.F., Engrand, C., Glavin, D.P., Bada, J.L., and Maurette, M.(1998) A search for extraterrestrial amino acids in carbonaceous Antarctic micrometeorites. *Orig Life Evol Biosph* 28:413–424.

Brownlee, D., Tsou, P., Aléon, J., Alexander, C.M.O.'D., Araki, T., Bajt, S., Baratta, G.A., Bastien, R., Bland, P., Bleuet, P., Borg, J., Bradley, J.P., Brearley, A., Brenker, F., Brennan, S., Bridges, J.C., Browning, N., Brucato, J.R., Brucato, H., Bullock, E., Burchell, M.J., Busemann, H., Butterworth, A., Chaussidon, M., Cheuvront, A., Chi, M., Cintala, M.J., Clark, B.C., Clemett, S.J., Cody, G., Colangeli, L., Cooper, G., Cordier, P.G., Daghlian, C., Dai, Z., D'Hendecourt, L.,

Djouadi, Z., Dominguez, G., Duxbury, T., Dworkin, J.P., Ebel, D., Economou, T.E., Fairey, S.A.J., Fallon, S., Ferrini, G., Ferroir, T., Fleckenstein, H., Floss, C., Flynn, G., Franchi, I.A., Fries, M., Gainsforth, Z., Gallien, J.-P., Genge, M., Gilles, M.K., Gillet, P., Gilmour, J., Glavin, D.P., Gounelle, M., Grady, M.M., Graham, G.A., Grant, P.G., Green, S.F., Grossemy, F., Grossman, L., Grossman, J., Guan, Y., Hagiya, K., Harvey, R., Heck, P., Herzog, G.F., Hoppe, P., Hörz, F., Huth, J., Hutcheon, I.D., Ishii, H., Ito, M., Jacob, D., Jacobsen, C., Jacobsen, S., Joswiak, D., Kearsley, A.T., Keller, L., Khodja, H., Kilcoyne, A.L.D., Kissel, J., Krot, A., Langenhorst, F., Lanzirotti, A., Le, L., Leshin, L., Leitner, J., Lemelle, L., Leroux, H., Liu, M.-C., Luening, K., Lyon, I., MacPherson, G., Marcus, M.A., Marhas, K., Matrajt, G., Meibom, A., Mennella, V., Messenger, K., Mikouchi, T., Mostefaoui, S., Nakamura, T., Nakano, T., Newville, M., Nittler, L.R., Ohnishi, I., Ohsumi, K., Okudaira, K., Papanastassiou, D.A., Palma, R., Palumbo, M.O., Pepin, R.E., Perkins, D., Perronnet, M., Pianetta, P., Rao, W., Rietmeijer, F., Robert, F., Rost, D., Rotundi, A., Ryan, R., Sandford, S.A., Schwandt, C.S., See, T.H., Schlutter, D., Sheffield-Parker, J.A., Simionovici, S., Sitnitsky, S.I., Snead, C.J., Spencer, M.K., Stadermann, F.J., Steele, A., Stephan, T., Stroud, R., Susini, J., Sutton, S.R., Taheri, M., Taylor, S., Teslich, N., Tomeoka, K., Tomioka, N., Toppani, A., Trigo-Rodríguez, J.M., Troadec, D., Tsuchiyama, A., Tuzzolino, A.J., Tyliszczak, T., Uesugi, K., Velbel, M., Vellenga, J., Vicenzi, E., Vincze, L., Warren, J., Weber, I., Weisberg, M., Westphal, A.J., Wirick, S., Wooden, D., Wopenka, B., Wozniakiewicz, P.A., Wright, I., Yabuta, H., Yano, H., Young, E.D., Zare, R.N., Zega, T., Ziegler, K., Zimmerman, L., Zinner, E., and Zolensky, M. (2006) Comet 81P/Wild 2 under a microscope. *Science* 314:1711–1716.

Burchell, M.J. (2012) Cratering on icy bodies. In *The Science of Solar System Ices*, edited by. M.S. Gudipati and J. Castillo-Rogez, Springer, New York, pp 253–278.

Burchell, M.J., Cole, M.J., McDonnell, J.A.M., and Zarnecki, J.C. (1999) Hypervelocity impact studies using the 2 MV Van de Graaff accelerator and two-stage light gas gun of the University of Kent. *Meas Sci Technol* 40:41–50.

Burchell, M.J., Mann, J., Bunch, A.W., and Brandão, P.F.B. (2001) Survivability of bacteria in hypervelocity impact. *Icarus* 154:545–547.

Burchell, M.J., Galloway, J.A., Bunch A.W., and Brandao, P. (2003) Survivability of bacteria ejected from icy surfaces after hypervelocity impact. *Orig Life Evol Biosph* 33:53–74.

Burchell, M.J., Mann, J.R., and Bunch, A.W. (2004) Survival of bacteria and spores under extreme pressures. *Mon Not R Astron Soc* 352:1273–1278.

Chyba, C. and Sagan, C. (1992) Endogenous production, exogenous delivery and impact-shock synthesis of organic molecules: an inventory for the origins of life. *Nature* 355:125–132.

Clemett, S.J., Maechling, C.R., Zare, R.N., and Swan, P.D. (1993) Identification of complex aromatic molecules in individual interplanetary dust particles. *Science* 262:721–725.

Cronin, J.R. (1989) Origin of organic compounds in carbonaceous meteorites. *Adv Space Res* 9:59–64.

Fendyke, S., Price, M.C., and Burchell, M.J. (2013) Hydrocode modelling of hypervelocity impacts on ice. *Adv Space Res* 52:705–714.

Flynn, G.J. (1996) The delivery of organic matter from asteroids and comets to the early surface of Mars. *Earth Moon Planets* 72:469–474.

Glavin, D.P., Dworkin, J.P., and Sandford, S.A. (2008) Detection of cometary amines in samples returned by Stardust. *Meteorit Planet Sci* 44:399–413.

Hayhurst, C.J. and Clegg, R.A. (1997) Cylindrical symmetric SPH simulations of hypervelocity impacts on thin plates. *Int J Impact Eng* 20:337–348.

Horneck, G., Stoffler, D., Eschweiler, U., and Hornemann, U. (2001) Bacterial spores survive simulated meteorite impact. *Icarus* 149:285–290.

Jerling, A., Burchell, M.J., and Tepfer, D. (2008) Survival of seeds in hypervelocity impacts. *International Journal of Astrobiology* 7:217–222.

Keller, L.P., Bajt, S., Baratta, G.A., Borg, J., Busemann, H., Brucato, J., Burchell, M., Colangeli, L., d'Hendecourt, L., Djouadi, Z., Ferrini, G., Flynn, G., Franchi, I.A., Fries, M., Grady, M.M., Graham, G.A., Grossemy, F., Kearsley, A., Matrajt, G., Mennell, V., Nittler, L., Palumbo, M.E., Rotundi, A., Sandford, S.A., Steele, A., Wooden, D., Wopenka, B., and Zolensky, M. (2006) Infrared spectroscopy of comet Wild-2 samples returned by the Stardust mission. *Science* 314:1728–1731.

Kyte, F.T. (2002) Unmelted meteoritic debris collected from Eltanin ejecta in *Polarstern* cores from expedition ANT XII/4. *Deep Sea Res Part 2 Top Stud Oceanogr* 49:1063–1071.

Laine, L. and Sandvik, A (2001). Derivation of mechanical properties for sand. In *Proceedings of the 4th Asia-Pacific Conference on Shock and Impact Loads on Structures,* CI-Premier, Singapore, pp 361–368.

Leighs, J.A., Hazell, P.J., and Appleby-Thomas, G.J. (2012) The effect of shock loading on the survival of plant seeds. *Icarus* 220:23–28.

LeVoci, G., Burchell, M.J., and Tepfer, D. (2009) Plant seed survival after impact into water at $1 \, \mathrm{km \, s^{-1}}$ [abstract 1239]. In *40th Lunar and Planetary Science Conference Abstracts*, Lunar and Planetary Institute, Houston.

Maier, W.D., Andreoli, M.A.G., McDonald, I., Higgins, M.D., Boyce, A.J., Shukolyukov, A., Lugmair, G.W., Ashwal, L.D., Gräser, P., Ripley, E.M., and Hart, R.J. (2006) Discovery of a 25-cm asteroid clast in the giant Morokweng impact crater, South Africa. *Nature* 441:203–206.

Managadze, G.G., Brinckerhoff, W.B., and Chumikov, A.E. (2003a) Molecular synthesis in hypervelocity impact plasmas on the primitive Earth and in interstellar clouds. *Geophys Res Lett* 30, doi:10.1029/2002GL016422.

Managadze, G.G., Brinckerhoff, W.B., and Chumikov, A.E. (2003b) Possible synthesis of organic molecular ions in plasmas similar to those generated in hypervelocity impacts. *Int J Impact Eng* 29:449–458.

Matrajt, G., Pizzarello, S., Taylor, S., and Brownlee, D. (2004) Concentration and variability of the AIB amino acid in polar micrometeorites: implications for the exogenous delivery of amino acids to the primitive Earth. *Meteorit Planet Sci* 39:1767–1894.

Matuska, D.A. (1984) *HULL Users' Manual,* Air Force Armament Laboratory document AFATL-TR-84-59, National Technical Information Service, Springfield, VA.

McKay, C.P. and Borucki, W.J. (1997) Organic synthesis in experimental impact shocks. *Science* 276:390–392.

Melosh, H.J. (1989) *Impact Cratering: A Geologic Process,* Oxford University Press, Oxford.

Milner, D.J., Burchell, M.J., Creighton, J.A., and Parnell, J. (2006) Oceanic hypervelocity impact events: a viable mechanism for successful panspermia? *International Journal of Astrobiology* 5:261–267.

Nna-Mvondo, D., Khare, B., Ishihara, T., and McKay, C.P. (2008) Experimental impact shock chemistry on planetary icy satellites. *Icarus* 194:822–835.

Parnell, J., Bowden, S., Lindgren, P., Burchell, M.J., Milner, D., Baldwin, E.C., and Crawford, I.A. (2010) The preservation of fossil biomarkers during hypervelocity impact experiments using organic rich siltstones as both projectiles and targets. *Meteorit Planet Sci* 45:1340–1358.

Peterson, E., Horz, F., and Chang, S. (1997) Modification of amino acids at shock pressures of 3.5 to 32 GPa. *Geochim Cosmochim Acta* 61:3937–3950.

Pierazzo, E. and Chyba, C.F. (1999) Amino acid survival in large cometary impacts. *Meteorit Planet Sci* 34:909–918.

Pierazzo, E. and Chyba, C.F. (2002) Cometary delivery of biogenic elements to Europa. *Icarus* 157:120–127.

Pierazzo, E. and Melosh, H.J. (2000a) Understanding oblique impacts from experiments, observations, and modeling. *Annu Rev Earth Planet Sci* 28:141–167.

Pierazzo, E. and Melosh, H.J. (2000b) Hydrocode modelling of oblique impacts: the fate of the projectile. *Meteorit Planet Sci* 35:117–130.

Price, M.C., Solscheid, C., Burchell, M.J., Jose, L., Adamek, N., and Cole, M.J. (2013) Survival of yeast spores in hypervelocity impact events up to velocities of $7.4\,\mathrm{km\ s^{-1}}$. *Icarus* 222:263–272.

Sandford, S.A. (2008) Terrestrial analysis of the organic component of comet dust. *Annu Rev Anal Chem (Palo Alto Calif)* 1:18.1–18.30.

Sandford, S.A., Aléon, J., Alexander, C.M.O.'D., Araki, T., Bajt, S., Baratta, G.A., Borg, J., Bradley, J.P., Brownlee, D.E., Brucato, J.R., Burchell, M.J., Busemann, H., Butterworth, A., Clemett, S.J., Cody, G., Colangeli, L., Cooper, G., D'Hendecourt, L., Djouadi, Z., Dworkin, J.P., Ferrini, G., Fleckenstein, H., Flynn, G.J., Franchi, I.A., Fries, M., Gilles, M.K., Glavin, D.P., Gounelle, M., Grossemy, F., Jacobsen, C., Keller, L.P., Kilcoyne, A.L.D., Leitner, J., Matrajt, G., Meibom, A., Mennella, V., Mostefaoui, S., Nittler, L.R., Palumbo, M.E., Papanastassiou, D.A., Robert, F., Rotundi, A., Snead, C.J., Spencer, M.K., Stadermann, F.J., Steele, A., Stephan, T., Tsou, P., Tyliszczak, T., Westphal, A.J., Wirick, S., Wopenka, B., Yabuta, H., Zare, R.N., and Zolensky, M.E. (2006) Organics captured from comet 81P/Wild 2 by the Stardust spacecraft. *Science* 314:1720–1724.

Senft, L.E. and Stewart, S.T. (2008) Impact crater formation in icy layered terrains on Mars. *Meteorit Planet Sci* 43:1993–2013.

Stöffler, D., Horneck, G., Ott, S., Hornemann, U., Cockell, C.S., Möller, R., Meyer, C., de Vera, J.-P., Fritz, J., and Artemieva, N.A. (2007) Experimental evidence for the potential impact ejection of viable microorganisms from Mars and Mars-like planets. *Icarus* 186:585–588.

Trunin, R.F., Gudarenko, L.F., Zhernokletov, M.V., and Simakov, G.V. (2001) Experimental data on shock compressibility and adiabatic expansion of condensed substances. *RFNC, Sarov* [in Russian]. Data taken from *Rusbank* database, http://teos.ficp.ac.ru/rusbank (accessed January 2013).

Willis, M.J., Ahrens, T.J., Bertani, L.E., and Nash, C.Z. (2006) Bugbuster—survivability of living bacteria upon shock compression. *Earth Planet Sci Lett* 247:185–196.

Zahnle, K., Schenk, P., Levison, H., and Dones, L. (2003) Cratering rates in the outer Solar System. *Icarus* 163:263–289.

Address correspondence to:
Professor Mark J. Burchell
School for Physical Sciences
Ingram Building
University of Kent
Canterbury, Kent CT2 7NH
UK

E-mail: m.j.burchell@kent.ac.uk